Journal of Alloys and Compounds 509 (2011) 3795–3805

Contents lists available at ScienceDirect

Journal of Alloys and Compounds

journal homepage: www.elsevier.com/locate/jallcom

The Al-rich region of the Al–Mn–Ni alloy system. Part II. Phase equilibria at 620–1000 °C

S. Balanetskyy[a,c,*], G. Meisterernst[b], B. Grushko[a], M. Feuerbacher[a]

[a] Institut für Festkörperforschung, Forschungszentrum Jülich, D-52425 Jülich, Germany
[b] Crystallography Section, Ludwig-Maximilians-Universität München, D-80333 München, Germany
[c] I.N. Frantsevich Institute for Problems of Materials Science, 03680 Kiev 142, Ukraine

ARTICLE INFO

Article history:
Received 23 July 2010
Received in revised form 20 October 2010
Accepted 23 October 2010
Available online 3 November 2010

Keywords:
Intermetallics
Ternary alloy systems
Phase identification

ABSTRACT

Phase equilibria in the Al-rich region of the Al–Mn–Ni alloy system were studied at 1000, 950, 850, 750, 700, 645 and 620 °C. Three ternary thermodynamically stable intermetallics, the φ-phase (Al_5Co_2-type, *hP26*, $P6_3/mmc$; $a = 0.76632(16)$, $c = 0.78296(15)$ nm), the κ-phase (κ-$Al_{14.4}Cr_{3.4}Ni_{1.1}$-type, *hP227*, $P6_3/m$; $a = 1.7625(10)$, $c = 1.2516(10)$ nm), and the O-phase (O-$Al_{77}Cr_{14}Pd_9$-type, *Pmmn*, *oP650*,: $a = 2.3316(16)$, $b = 1.2424(15)$, $c = 3.2648(14)$ nm), as well as three ternary metastable phases, the decagonal D_3-phase with periodicity about 1.25 nm, the $Al_9(Mn,Ni)_2$-phase (Al_9Co_2-type, $P112_1/a$, mP22; $a = 0.8585(16)$, $b = 0.6269(9)$, $c = 0.6205(11)$ nm, $\beta = 95.34(10)^\circ$) and the O_1-phase (*base-centered orthorhombic*, $a \approx 23.8$, $b \approx 12.4$, $c \approx 32.2$ nm) were revealed. Their physicochemical behaviour in the Al–Mn–Ni alloy system was studied.

1. Introduction

Al–Mn–Ni belongs to the alloy systems, in which structurally complex metallic alloys (CMAs, see definition in [1]) and quasicrystals (QC) are formed. The phase equilibria in this system have not been fully characterized up to now, which is surprising, particularly because Al, Mn, and Ni, as well as their alloys, are widely used in industry.

Phase equilibria in the Al-rich region of the Al–Mn–Ni alloy system (from 85 to 100 at.% Al) were firstly investigated by Raynor [2]. In that work, the partial liquidus surface, isothermal sections at 500, 600 and 630 °C as well as several polythermal sections were determined. Besides the binary intermetallics Al_6Mn, Al_4Mn, and Al_3Ni, two ternary phases, termed X and Y were reported. While the X-phase, $Al_{60}Mn_{11}Ni_4$, was reported as thermodynamically stable (*Bbmm*, *oS156*, $Al_{31}Mn_6Ni_2$: $a = 2.388$, $b = 1.243$, and $c = 0.778$ nm [7]), Y as metastable.

Later works on this system addressed only the phase equilibria in the TM-rich region (TM = transition metals) from 0 to 50 at.% Al [3,4] and in from 0 to 70 at.% Al [5]. According to [3], above 840 °C the congruent β-AlNi phase (B2-structure) and γ-AlMn of the W-type (A2-structure) form a continuous range (β), since the B2 ↔ A2 transformation in the Al-rich region of Al–Mn–Ni takes place via a second-order phase transition. Therefore, at high temperatures, the Al-rich region of Al–Mn–Ni may formally be considered independent from other parts of the system.

The situation with the thermodynamically stable intermediate phases in the Al-rich region of Al–Mn–Ni is described in detail in part one of this study [6]. In this paper, we report on the phase equilibria and the ternary metastable phases observed in the system Al–Mn–Ni.

2. Experimental procedure

Alloys were produced from the constituent elements by levitation induction melting in a water-cooled copper crucible under Ar atmosphere. The purity of Al was 99.999%, of Mn 99.99%, and of Ni 99.99%. The weight of the ingots was typically about 5 g. Parts of the samples were annealed under Ar atmosphere or vacuum for up to 958 h and subsequently water-quenched. Mechanically grinded and polished samples were investigated by scanning electron microscopy (SEM) and the phase compositions were measured by energy-dispersive X-ray analysis (EDX) in SEM. The composition of selected samples was determined by inductively coupled plasma optical emission spectroscopy. These analyses were used for calibrating the EDX measurements. The samples were further studied by selected area electron diffraction (SAED) in a JEOL 4000FX transmission electron microscope (TEM) operated at 400 kV. The TEM samples were powders spread on Cu grids covered by carbon films or thinned by mechanical grinding and subsequent ion-beam milling. Powder X-ray diffraction (PXRD) was carried out on a STOE diffractometer in transmission mode. We used Mo $K_{\alpha 1}$ radiation and a position-sensitive detector. Patterns were taken between $4^\circ \le 2\Theta \le 54^\circ$ with a step width of $\Delta 2\Theta = 0.02^\circ$. Differential thermal analysis (DTA) of selected samples was carried out with heating and cooling rates of 2.0 K/min.

* Corresponding author at: Maxim-Gorki-Str. 12, D-09599 Freiberg.
E-mail address: dr.balanetskyy@alice-dsl.net (S. Balanetskyy).

0925-8388/$ – see front matter © 2010 Elsevier B.V. All rights reserved.
doi:10.1016/j.jallcom.2010.10.114

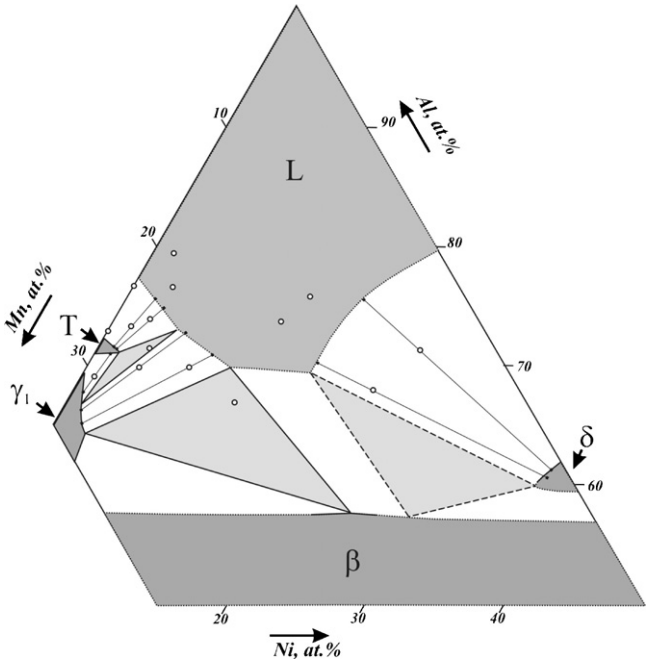

Fig. 1. Partial isothermal section at 1000 °C. The compositions of the alloys studied are marked by circles. Suggested three-phase equilibria are marked by dashed lines, the estimated borders of single-phase fields are marked by dotted lines.

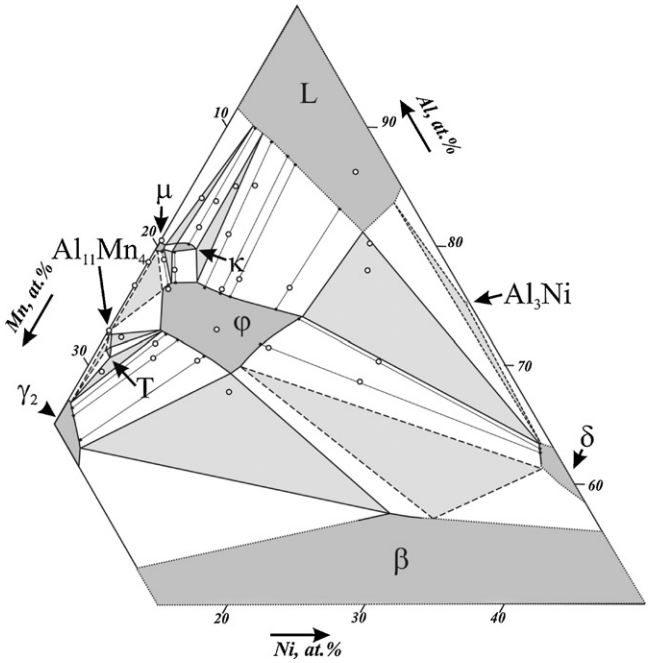

Fig. 3. Partial isothermal section at 850 °C.

3. Results and discussions

3.1. Isothermal sections

Partial isothermal sections of the Al-rich part of Al–Mn–Ni alloy system between 1000 and 620 °C are shown in Figs. 1–7, the composition, heat treatments durations and phase content of the alloys studied are shown in Appendix A. In the following, we will describe our findings, starting from the highest temperatures. The data on the phase equilibria in the binary Al–Mn and Al–Ni alloy systems are taken from [8]. Crystallographic data of the Al-rich Al–Mn–Ni phases according to part one of this study [6] and literature data are provided in Table 1. The metallurgical characteristics (sample composition, annealing parameters, composition of phases observed) of all samples studied are provided in Appendix A.

At *1000 °C* (Fig. 1) ternary phases in the Al-rich region of Al–Mn–Ni do not exist. The binary T-phase solves up to ~1.7 at.% Ni at ~71.2 at.% Al and coexists in equilibrium with γ_1, and the liquid (L), which occupies a significant part of this section. The γ_1-phase solves up to ~3.0 at.% Ni at ~63.2 at.% Al and in addition to equilibria with T and L coexists also with the β-phase. The latter coexists also in equilibrium with the δ-phase, which solves up to ~3.3 at.% Mn at ~60.0 at.% Al at this temperature.

At *950 °C* (Fig. 2) the ternary hexagonal φ-phase, forming at about 993 °C according to DTA, is already present in the system. At this temperature, it is located within the

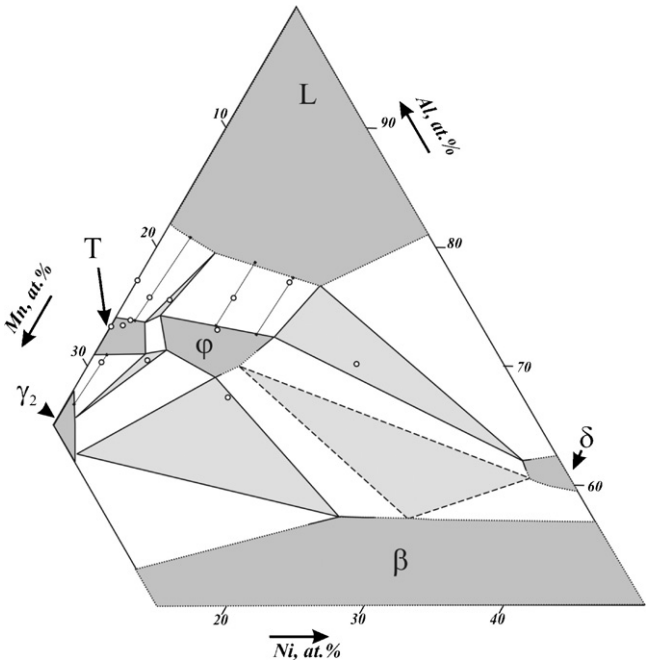

Fig. 2. Partial isothermal section at 950 °C.

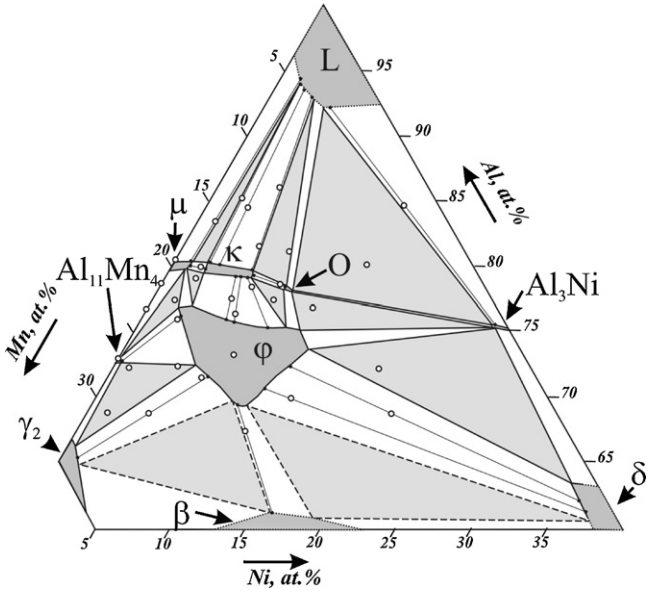

Fig. 4. Partial isothermal section at 750 °C.

Table 1
Crystallographic data of the thermodynamically stable Al-rich phases of Al–Mn–Ni (see [6]).

Designation of phase		Space group or Bravais lattice, Pearson symbol, structure type	Lattice parameters		
In this work	Other		*a*, nm *α*,°	*b*, nm *β*,°	*c*, nm *γ*,°
Binary phases					
β-Al(Mn, Ni)	γ-(AlMn)	*Im3̄m* *cI2* W	0.3063 –	– –	– –
	β-(AlNi)	*Pm3̄m* *cP2* CsCl	0.2848 –	– –	– –
γ_1	*h*-Al_8Mn_5	*I43̄m* *cI52* *h*-Al_8Cr_5	0.8890 –	– –	– –
γ_2	l-Al_8Mn	*R3̄m* *hR26* R-Al_8Cr_5	0.90508 89.273	– –	– –
T	Al_3Mn $Al_{11}Mn_4$ (HT) *H*	*Pnma or Pna 2₁* *oP156* *Al_3Mn*	1.4789	1.2460	1.2562
μ	μ-Al_4Mn	$P6_3/mmc$ *hP563* *μ-Al_4Mn*	2.0015	–	2.4699
$Al_{11}Mn_4$	Al_3Mn $Al_{11}Mn_4$ (LT) *R*	*P1* *aP30* $Al_{11}Mn_4$	0.5095 89.35	0.8879 100.47	0.5051 105.08
δ	Al_3Ni_2	*P3̄m1* *hP5* Al_3Ni_2	0.4036 –	– –	0.4897 –
Al_3Ni	Al_3Ni	*Pnma* *oP16* CF_3	0.6598	0.7352	0.4802
Ternary phases					
κ	ζ	$P6_3/m$ *hP227* κ-$Al_{14.4}Cr_{3.4}Ni_{1.1}$	1.7625	–	1.2516
φ	–	$P6_3/mmc$ *hP26* Al_5Co_2	0.76632	–	0.78296
O	$C_{3,l}$	*Pmmn* *oP650* O-$Al_{77}Cr_{14}Pd_9$	2.3316	1.2424	3.2648

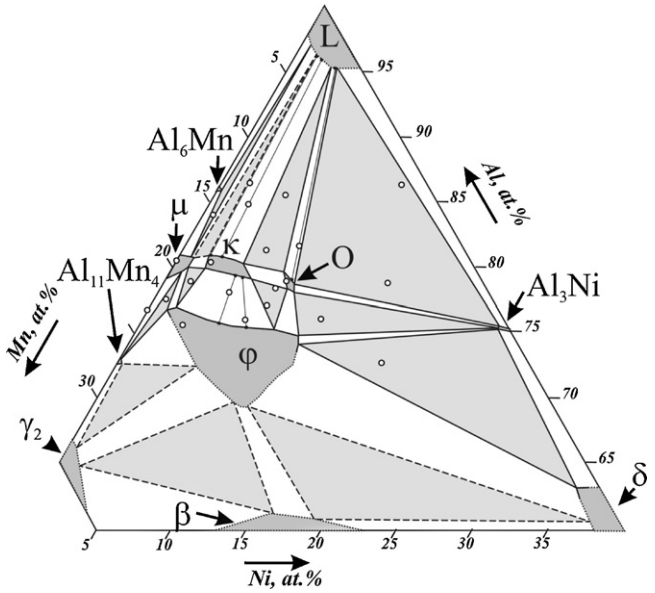

Fig. 5. Partial isothermal section at 700 °C.

compositional region spanned by ~$Al_{71.5}Mn_{23.3}Ni_{5.0}$, $Al_{74.4}Mn_{22.6}Ni_{3.0}$, $Al_{72.5}Mn_{15.3}Ni_{12.2}$, and $Al_{69.2}Mn_{21.2}Ni_{9.6}$, and coexists with the T, γ_2-, β-, and δ-phase as well as with the liquid. The binary T-phase solves up to ~3.5 at.% Ni at ~71.0 at.% Al and γ_2 up to ~2.8 at.% Ni at ~63.2 at.% Al. The maximum content of Al in the β-phase was determined as ~57.4 at.% at ~24.6 at.% Ni. The δ-phase solves up to ~2.7 at.% Mn at ~62.1 at.% Al.

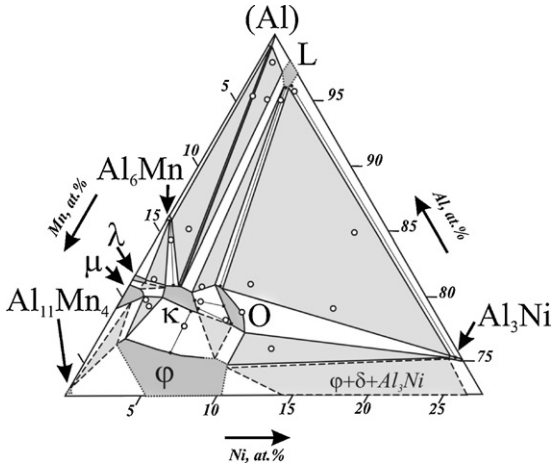

Fig. 6. Partial isothermal section at 645 °C.

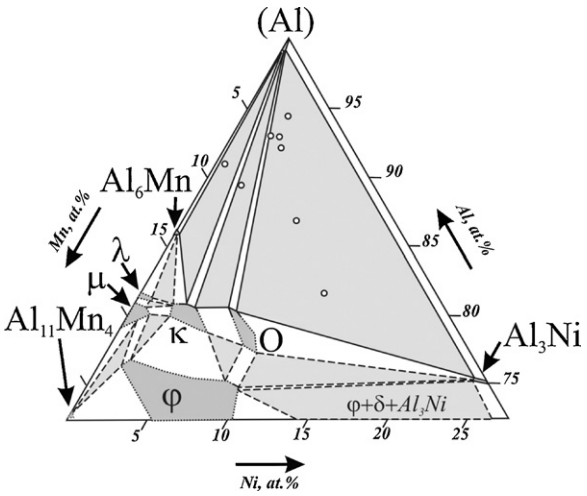

Fig. 7. Partial isothermal section at 620 °C.

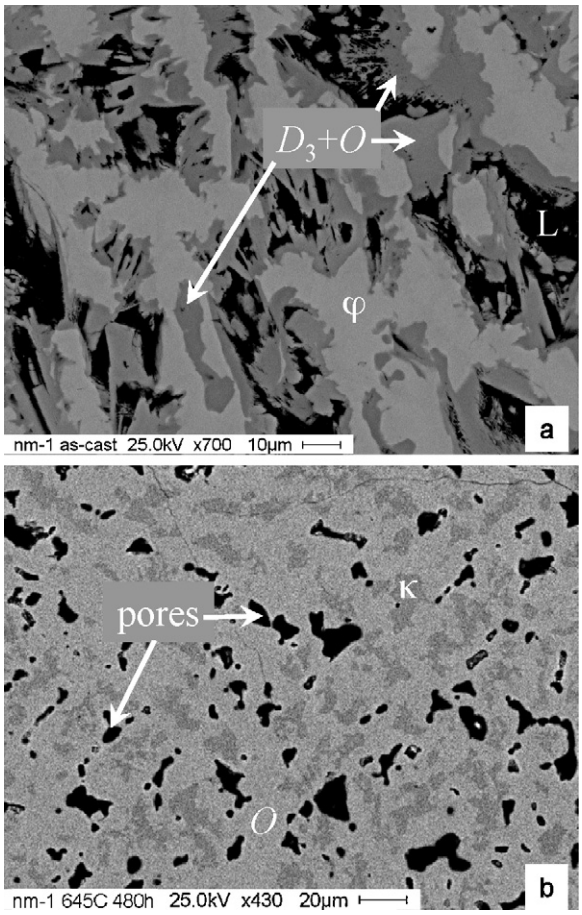

Fig. 8. SEM micrographs of the as-cast $Al_{79.6}Mn_{15.1}Ni_{5.3}$ alloy (a), and of the same alloy (b) after annealing at 645 °C for 480 h (Sample No 109 in Appendix A). The φ-phase in (a) has the composition $Al_{75.1}Mn_{19.2}Ni_{5.7}$. Since the compositions of D_3 and O are very close and can not be distinguished, the dark-grey phase with composition ranging from $Al_{80.8}Mn_{13.9}Ni_{5.3}$ to $Al_{80.3}Mn_{13.3}Ni_{6.4}$ in is labelled (D_3 + O). The solidified liquid L of composition $Al_{97.4}Mn_{1.2}Ni_{1.4}$ contains mainly (Al) and ((Al) + Al_3Ni) eutectic.

At *850 °C* (Fig. 3), in addition to the φ-phase, the ternary hexagonal κ-phase, forming at about 867 °C according to DTA, shows up in the system. At this temperature, it has a relatively small homogeneity region located along the line between the compositions ~$Al_{80.0}Mn_{18.8}Ni_{1.2}$ and $Al_{79.8}Mn_{17.2}Ni_{3.0}$ and coexists with φ, μ and the liquid. The homogeneity region of φ at 850 °C is located within the range spanned by $Al_{73.0}Mn_{23.4}Ni_{3.6}$, $Al_{77.5}Mn_{19.8}Ni_{2.7}$, $Al_{74.1}Mn_{12.5}Ni_{13.4}$, and $Al_{69.4}Mn_{20.0}Ni_{10.6}$, i.e. it is significantly enriched in Al and Ni with respect to the situation at 950 °C. The solubility of Ni in the binary triclinic $Al_{11}Mn_4$ phase (a low-temperature modification of the orthorhombic T-phase) and in the hexagonal μ-phase is practically negligible (~0.5 at.%, which is comparable with the experimental uncertainty of our EDX system). The maximum solubility of Ni in γ_2 is practically the same as at 950 °C. The maximum content of Al in the β-phase is about 57.6 at.% at ~28.0 at.% Ni, i.e. it is shifted to the Ni-richer region comparing to the situation at 950 °C. The δ-phase solves up to ~1.6 at.% Mn at ~61.5 at.% Al. At 850 °C. The T-phase is not a stable phase in the binary Al–Mn system anymore [8]. Its homogeneity region, which due to stabilization by Ni is still present in a small compositional region around ~$Al_{71.5}Mn_{27.5}Ni_{1.0}$, has no connection to binary Al–Mn anymore. At 850 °C, the T-phase coexists in equilibrium with γ_2, ($Al_{11}Mn_4$) and φ.

At *750 °C* (Fig. 4) another ternary intermetallic, the orthorhombic O-phase occurs in the Al–Mn–Ni alloy system forming at about 757 °C according to DTA. At this temperature, it has a very small homogeneity region located around the composition ~$Al_{78.5}Mn_{13.0}Ni_{8.5}$ and coexists with φ, κ, Al_3Ni and the liquid. The homogeneity region of φ at 750 °C is located within the range spanned by $Al_{72.5}Mn_{22.2}Ni_{5.3}$, $Al_{76.9}Mn_{21.1}Ni_{2.0}$, $Al_{73.6}Mn_{14.2}Ni_{12.2}$ and $Al_{69.3}Mn_{21.1}Ni_{9.6}$, i.e. it is slightly smaller with respect to the situation at 850 °C. The κ-phase has a larger homogeneity region than at 850 °C and is located along the line between the compositions $Al_{80.0}Mn_{17.7}Ni_{2.3}$ and $Al_{79.4}Mn_{14.8}Ni_{5.8}$, i.e. it is significantly enriched in Ni. The T-phase is already absent in the Al–Mn–Ni alloy system at 750 °C. The maximum solubility of Ni in $Al_{11}Mn_4$ of ~0.5 at.% is practically identical as at 850 °C, but the Ni content in the μ-phase reaches ~1.5 at.%, which is significantly higher than at 850 °C. The maximum solubility of Mn in δ is ~2.0 at.%, and in (Al_3Ni) ~1.0 at.%. The maximum content of Al in the β-phase was determined as ~61.0 at.% at ~16.2 at.% Ni.

At *700 °C* (Fig. 5) the binary Al_6Mn-phase appears in the Al–Mn–Ni alloy system. The solubility of Ni in this phase is about 0.5 at.%. The μ-phase solves up to ~1.0 at.% Ni, a value slightly smaller than that at 750 °C. The solubility of Ni in ($Al_{11}Mn_4$) again is practically negligible. The binary (Al_3Ni) and δ-phase solve up to ~1.0 and 1.5 at.% Mn, respectively. At 700 °C the same ternary phases as at 750 °C are found, but their compositional regions differ slightly. The κ-phase is located within the compositional region spanned by $Al_{80.0}Mn_{17.8}Ni_{2.2}$, $Al_{81.0}Mn_{18.0}Ni_{2.0}$, $Al_{80.3}Mn_{15.1}Ni_{4.6}$, and $Al_{79.0}Mn_{15.2}Ni_{5.8}$. The homogeneity region of the O-phase is significantly wider, and is located along the line between the compositions ~$Al_{78.0}Mn_{13.0}Ni_{9.0}$ and $Al_{79.6}Mn_{12.9}Ni_{7.5}$. The homogeneity region of the φ-phase was studied only at its Al-rich limit. It was established that a decrease in temperature from 750 to 700 °C is accompanied by a diminishment of its homogeneity region. At this temperature its Al-rich region is located within the range spanned by $Al_{77.0}Mn_{21.5}Ni_{1.5}$, $Al_{75.2}Mn_{15.7}Ni_{9.1}$, and $Al_{74.0}Mn_{14.5}Ni_{11.5}$.

At *645 °C* (Fig. 6) the liquid occupies a very small compositional region close to the Al-rich side of the binary Al–Ni system and (Al) is already solid. The maximum solubility of Mn in aluminium is ~0.7 at.% and of Ni in aluminium is ~0.2 at.%, i.e. it is practically negligible. The binary λ-phase occurs in the system dissolving up to ~1.0 at.% Ni. The solubility of Ni in (Al_6Mn) and μ, as well as the solubility of Mn in (Al_3Ni) is practically the same as at 700 °C. The compositional region of the κ-phase is also similar with that at 700 °C but a little richer in Al. The homogeneity range of the O-phase continues expansion and is located along the line between the compositions ~$Al_{77.4}Mn_{13.2}Ni_{9.4}$ and $Al_{81.0}Mn_{13.4}Ni_{5.6}$. At the same time, the homogeneity range of the φ-phase continues con-

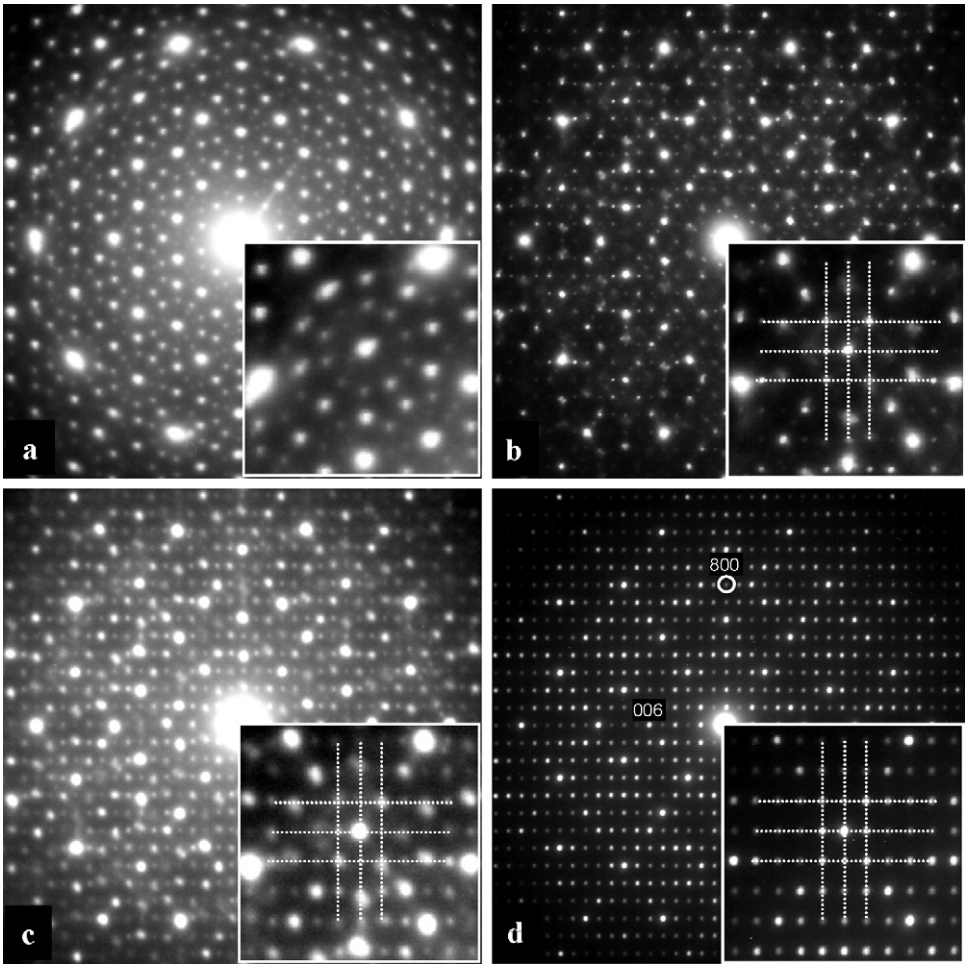

Fig. 9. SAED patterns in the as-cast $Al_{79.6}Mn_{15.1}Ni_{5.3}$ alloy. D_3 along the 10-fold axis (a), distorted D_3 along the 10-fold axis (b), distorted O along [0 1 0] (c). Perfect O-phase along [0 1 0] (d) in the same alloy after annealing at 645 °C for 480 h (Sample No 109 in Appendix A). Enlarged fragments of the patterns are shown in the insets. Grids in (b) and (c) correspond to perfect spot positions.

traction. Its Al-rich region is located within the range spanned by $Al_{76.8}Mn_{21.4}Ni_{1.8}$ and $Al_{74.9}Mn_{15.6}Ni_{9.5}$.

At *620 °C* (Fig. 7) the liquid phase is absent in the system. The existing solid phases are the same as at 645 °C. The κ-phase coexists in equilibrium with Al_6Mn, (Al) and O and, the O-phase coexists with (Al_3Ni) and (Al). All other equilibria were extrapolated from higher temperatures.

3.2. Metastable phases

The existence of a thermodynamically stable R-phase of stoichiometry $Al_{60}Mn_{11}Ni_4$ was reported in [2] (therein referred to as X-phase). However, in later work [9,10] other phases were attributed to that stoichiometry (see Table 2). Small amounts of R were reported to coexist with the distorted decagonal phase (D_3) and the O-phase (C_{3l}) in as-cast samples in [11]. In consistency with the later work [9,10] and in discrepancy with [2], our investigations provide evidence that above 620 °C a thermodynamically stable R-phase is not present in the Al–Mn–Ni alloy system.

The microstructure of the as-cast $Al_{79.6}Mn_{15.1}Ni_{5.3}$ alloy in Fig. 8a shows a phase (dark-grey) of composition close to $Al_{60}Mn_{11}Ni_4$, which coexists with the φ-phase (bright-grey) and a mixture of (Al) and ((Al) + Al_3Ni) eutectic (black). SAED investigations (Fig. 9a–c) show that the dark-grey area is not R-phase, but a mixture of distorted decagonal D_3-phase and distorted O-phase. In Fig. 9c, one can clearly see zigzag deviations of reflections from ideal positions, which is typical of the phason-like defects of the distorted O-phase [9]. For comparison diffraction pattern of the perfect D_3- and O-phase are shown in Fig. 9a and d, respectively. In these patterns the rows of reflections are perfectly aligned. In a few grains of distorted D_3-phase, it was possible using the smallest available aperture to find regions where this phase was nearly perfect (as shown in Fig. 9a). In most cases, however, this was impossible even with the smallest available aperture. In these regions, the distorted D_3-phase was identified as a fine mixture of D_3-phase and distorted O, but the individual domains were too small for separate investigation. Therefore one can see reflections typical of both constituents in Fig. 9b.

We have carried out additional annealings of 65 h at 800 °C with subsequent water quenching at compositions around $Al_{60}Mn_{11}Ni_4$. We find no occurrence of the R-phase and the same phases in equilibrium as at 850 °C.

After annealing of the $Al_{86.8}Mn_{6.1}Ni_{7.1}$ sample at 645 °C for 480 h, two constituents were found (Fig. 8b), the κ-phase and the O-phase (Fig. 9d). Both phases have compositions close to the $Al_{60}Mn_{11}Ni_4$ stoichiometry, and both are of good structural quality. Furthermore, dark contrast due to the presence of pores is seen. The DTA heating runs of the sample shows no according thermal effects between 500 and 758 °C, and hence we can exclude that the pores were filled with residual melt prior to sample preparation.

Table 2
Literature crystallographic data for the Al–Mn–Ni ternary-phases with compositions close to $Al_{60}Mn_{11}Ni_4$.

Designation of phase		Space group, Pearson symbol, structure type	Lattice periods, nm			Alloy composition	State of alloys	Ref.
This work	Other		*a*	*b*	*c*			
R	X $Al_{60}Mn_{11}Ni_4$	*Bbmm* *oS156* $Al_{31}Mn_6Ni_2$	2.388	1.243	0.778	$Al_{80.0}Mn_{14.7}Ni_{5.3}$[a]	Annealed at 500, 600 and 630 °C up to ~1200 h	[2,7]
O	$C_{3,I}$	Orth	2.40	1.24	3.27	$Al_{80.0}Mn_{14.7}Ni_{5.3}$	As-cast, annealed at 400 °C for 100 h	[9,11]
–	$C_{3,II}$[b]	Orth.	1.31	1.24	2.66	$Al_{80.0}Mn_{14.7}Ni_{5.3}$	Annealed at 400 °C for 100 h	[9]
D_3	T_3	Decagonal	–	1.24	–	$Al_{80.0}Mn_{14.7}Ni_{5.3}$	Rapidly solidified, as-cast	[9–11]
–	T	*I-centred orth* – –	1.24	1.26	3.14	$Al_{80.0}Mn_{14.7}Ni_{5.3}$	Annealed at 600 °C for 2 h	[10]

[a] Phase composition.
[b] May also be represented in related monoclinic system [9].

Since all phases listed in Table 2 except the O-phase were not found in the samples annealed at 620–1000 °C (see Appendix A), we conclude that all these phases are metastable in the temperature region studied. Vice versa, since annealing significantly improves the structural quality of the O-phase, we conclude that this phase is thermodynamically stable.

Microstructural analysis of the as-cast $Al_{82.6}Mn_{10.4}Ni_{7.0}$, $Al_{85.5}Mn_{2.2}Ni_{12.3}$ and $Al_{86.8}Mn_{6.1}Ni_{7.1}$ alloys revealed a phase with a composition of about $Al_{82.5}Mn_{2.8}Ni_{14.7}$. This composition is very close to Al_9TM_2 (where *TM* stands for transition metals). Phases of Al_9Co_2-structure type [12] exist also in other systems, e.g. Al_9Ni_2 (metastable) [12] and $Al_9(TM,Ni)_2$ (TM = Fe, Ru) [13,14]. Therefore we suggest that $Al_{82.5}Mn_{2.8}Ni_{14.7}$ also is of Al_9Co_2-type structure. In contrast to $Al_9(Fe,Ni)_2$ and $Al_9(Ru,Ni)_2$, however, this phase turned out to be metastable in the studied temperature region, i.e. it was not found in any of the annealed or slowly solidified samples. Therefore it was impossible to produce single-phase $Al_9(Mn,Ni)_2$ samples, and we resorted to as-cast $Al_{86.8}Mn_{6.1}Ni_{7.1}$ samples, which contain a large amount of the required phase (Fig. 10), for structure identification. The $Al_9(Mn,Ni)_2$-phase was found to be unstable under the electron beam, impeding structural analysis by means of electron diffraction in the TEM. We hence compared a PXDR pattern of the $Al_{86.8}Mn_{6.1}Ni_{7.1}$ sample with a calculated pattern for the Al_9Ni_2-structure (Fig. 11). The theoretical pattern was calculated using the model for Al_9Co_2 [15], where Co atoms were replaced by

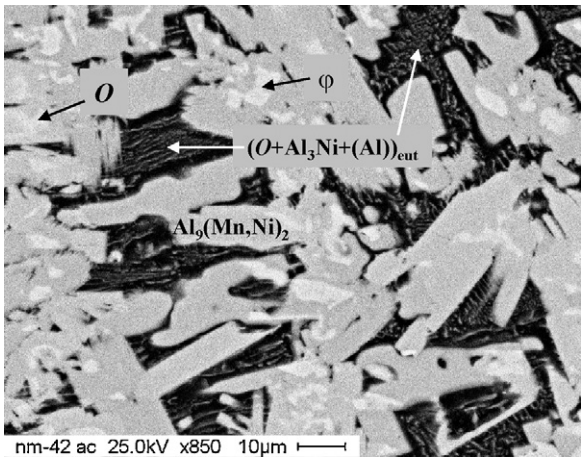

Fig. 10. SEM micrograph of the as-cast $Al_{86.8}Mn_{6.1}Ni_{7.1}$ alloy.

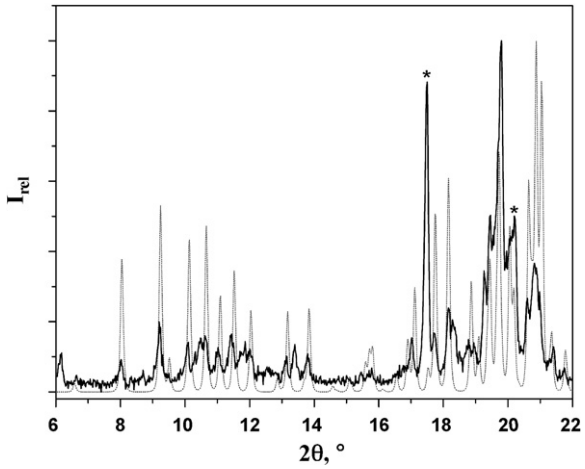

Fig. 11. PXRD pattern of the as-cast $Al_{86.8}Mn_{6.1}Ni_{7.1}$ alloy (solid line) in comparison with the calculated pattern for Al_9Ni_2 (dashed line). The reflections labeled with an asterisk belong to (Al). Reflections, which do not coincide with the calculated Al_9Ni_2 reflections and those of (Al), belong to the (- and O-phases [6].

Ni. We find clear coincidences between the experimental and calculated pattern, indicating that the $Al_9(Mn,Ni)_2$-structure is indeed present in the alloy. Further reflections of (Al), φ and O are also present, which is consistent with SEM-EDX and TEM investigations of the $Al_{86.8}Mn_{6.1}Ni_{7.1}$ sample (Fig. 10). The extracted peak-file of the $Al_9(Mn,Ni)_2$-phase was indexed using the structural parameters $P112_1/a$, mP22, Al_9Co_2-type; $a = 0.8585(16)$; $b = 0.6269(9)$, $c = 0.6205(11)$ nm, $\beta = 95.34(10)°$. It should furthermore be mentioned that traces of a base-centered orthorhombic phase ($a \approx 23.8$, $b \approx 12.4$, $c \approx 32.2$ nm) similar to O_1-Al–Cr–Fe [16] were also found in this alloy by TEM. This phase was also found to be metastable and is hence completely absent in the equilibrated samples.

Acknowledgements

We thank C. Thomas, M. Schmidt, and E.-M. Würtz for technical contributions and M. Heggen, S. Roitsch, S. Mi and T. Ya. Velikanova for helpful discussions. This work was financially supported by the DFG (project Ur51/8-2) and the 6th Framework EU Network of Excellence "Complex Metallic Alloys" (Contract No. NMP3-CT-2005-500140).

Appendix A. Metallurgical characteristics of Al–Mn–Ni alloys studied at 1000–620 °C.

No	Composition of alloy, at.%			Duration of heat treatment, h	Phase(s) in equilibrium	Phase composition, at.%		
	Al	Mn	Ni			Al	Mn	Ni
1000 °C								
1	73.0	27.0	–	64	T	72.3	27.7	–
					L	~77.5	~22.5	–
2	76.8	23.2	–	64	T	72.3	27.7	–
					L	~77.5	~22.5	–
3	69.2	29.0	1.8	94	T	71.1	27.9	1.0
					γ_1	67.6	31.6	0.8
4	73.4	25.2	1.4	94	T	71.6	27.4	1.0
					L	~75.8	~22.0	~2.2
5	74.0	23.5	2.5	94	T	71.4	27.2	1.4
					L	~75.2	~21.7	~3.1
6	76.7	20.5	2.8	94	L	76.7	20.5	2.8
7	79.5	19.0	1.5	94	L	79.5	19.0	1.5
8	71.5	24.8	3.7	94	T	71.1	27.2	1.7
					γ_1	67.0	32.0	1.0
					L	~73.5	~21.0	~5.5
9	70.0	26.3	3.7	94	γ_1	66.4	32.3	1.3
					L	~73.2	~21.0	~5.8
10	70.0	22.7	7.3	94	γ_1	65.3	32.9	1.8
					L	~70.8	~20.7	~8.5
11	66.9	20.9	12.2	94	β	57.7	17.2	25.1
					γ_1	64.4	33.0	2.6
					L	~69.6	20.3	~9.8
12	73.6	14.3	12.1	94	L	73.6	14.3	12.1
13	75.7	11.1	13.2	94	L	75.7	11.1	13.2
14	68.0	10.4	21.6	94	δ	60.6	1.9	37.5
					L	~70.2	13.2	~16.6
15	71.4	5.2	23.4	94	δ	61.2	1.0	37.8
					L	~75.6	7.3	~17.1
950 °C								
16	73.5	26.5	–	118	T	74.2	25.8	–
					L	~82.0	~18.0	–
17	77.3	22.7	–	118	T	74.2	25.8	–
					L	~82.0	~18.0	–
18	70.5	27.8	0.8	118	T	71.0	28.1	0.9
					γ_2	67.2	32.3	0.5
19	73.5	25.7	0.8	118	T	73.5	25.7	0.8
20	74.0	24.8	1.2	118	T	74.0	24.8	1.2
21	75.8	22.6	1.6	118	T	73.9	24.7	1.4
					L	~80.9	~17.1	~2.0
22	75.7	21.3	3.0	118	T	73.8	23.9	2.3
					φ	74.4	22.6	3.0
					L	~79.5	16.0	4.5
23	70.6	25.3	4.1	118	T	71.1	25.3	3.6
					φ	71.4	23.7	4.9
					γ_2	65.7	33.1	1.2
24	75.8	16.6	7.6	118	φ	73.5	19.0	7.5
					L	~78.5	~13.8	~7.7
25	73.1	19.1	7.8	118	φ	73.1	19.1	7.8
26	67.5	21.1	11.4	118	φ	69.0	21.4	9.6
					β	57.5	18.2	24.3
					γ_2	62.7	34.6	2.7
27	77.1	11.9	11.0	118	φ	72.8	16.6	10.7
					L	~77.5	~11.5	~11.0
28	70.2	10.6	19.2	118	φ	72.5	15.3	12.2
					δ	62.1	2.7	35.2
					L	~76.7	~9.9	~13.4
850 °C								
29	72.8	27.2	–	118	$Al_{11}Mn_4$	72.8	27.2	–
30	76.6	23.4	–	118	$Al_{11}Mn_4$	73.1	26.9	–
					μ	79.6	20.4	–
31	78.7	21.3	–	118	$Al_{11}Mn_4$	73.1	26.9	–
					μ	79.6	20.4	–
32	80.6	19.4	–	118	μ	80.4	19.6	–
					L	~91.5	~8.5	–
33	72.4	26.4	1.2	139	$Al_{11}Mn_4$	72.6	26.9	0.5
					T	71.6	27.5	0.9
					φ	73.0	23.4	3.6
34	69.7	29.1	1.2	167	T	70.7	28.3	1.0
					φ	72.9	23.3	3.8
					γ_2	67.0	32.8	0.2
35	71.9	24.2	3.9	135	φ	72.6	23.2	4.2
					γ_2	66.6	32.9	0.5

Appendix (*Continued*)

No	Composition of alloy, at.%			Heat treatment, °C/h	Phase(s) in equilibrium	Phase composition, at.%		
	Al	Mn	Ni			Al	Mn	Ni
36	70.6	25.1	4.3	167	φ	72.1	22.5	5.4
					γ_2	65.9	33.2	0.9
37	70.4	22.0	7.6	139	φ	70.8	21.3	7.9
					γ_2	63.9	33.6	2.5
38	67.8	20.9	11.3	167	φ	69.4	20.0	10.6
					β	57.6	14.4	28.0
					γ_2	63.1	33.9	3.0
39	71.6	16.2	12.2	140	φ	71.9	16.6	11.5
					δ	62.6	1.2	36.2
40	68.9	11.6	20.2	139	φ	72.0	16.4	11.6
					δ	62.9	1.0	36.1
41	70.4	8.9	20.7	139	φ	74.0	12.9	13.1
					δ	63.1	1.0	35.9
42	78.1	5.8	16.1	139	φ	74.1	12.5	13.4
					δ	63.4	0.8	35.8
					L	~81.3	~4.6	~14.1
43	73.1	19.1	7.8	135	φ	73.1	19.1	7.8
44	76.4	21.0	2.6	118	φ	76.4	21.0	2.6
45	78.9	20.1	1.0	139	φ	76.9	20.7	2.4
					μ	79.6	19.9	0.5
46	78.2	19.6	2.2	135	φ	77.5	19.8	2.7
					κ	79.6	18.9	1.5
47	84.1	14.8	1.1	167	μ	80.2	19.3	0.5
					κ	80.4	18.3	1.3
					L	~90.0	8.2	~1.8
48	81.6	16.2	2.2	118	κ	80.3	17.6	2.1
					L	~89.8	~8.0	~2.2
49	83.8	13.8	2.4	167	κ	80.3	17.5	2.2
					L	~89.7	~7.8	~2.5
50	85.1	11.8	3.1	118	κ	79.9	17.1	3.0
					φ	77.0	18.7	4.3
					L	~89.5	~7.5	~3.0
51	81.1	14.3	4.6	118	φ	76.6	18.4	5.0
					L	~88.8	~7.3	~3.9
52	85.1	10.5	4.4	118	φ	76.6	18.3	5.1
					L	~88.5	~7.4	~4.1
53	76.5	17.1	6.4	167	φ	76.1	17.4	6.5
					L	~87.5	~7.0	~5.5
54	77.3	15.4	7.3	135	φ	75.7	17.0	7.3
					L	~77.0	~16.5	~6.5
55	76.6	12.2	11.2	167	φ	74.7	14.1	11.2
					L	~83.0	~5.5	~11.5
750 °C								
56	73.2	26.8	–	161	$Al_{11}Mn_4$	73.2	26.8	–
57	76.7	23.3	–	161	$Al_{11}Mn_4$	73.2	26.8	–
					μ	79.6	20.4	–
58	80.6	19.4	–	181	μ	80.3	19.7	–
					L	~96.0	~4.0	–
59	72.2	26.7	1.1	90	$Al_{11}Mn_4$	72.6	26.9	0.5
					φ	72.5	22.2	5.3
					γ_2	66.3	33.2	0.5
60	72.2	23.5	4.3	161	$Al_{11}Mn_4$	72.6	26.9	0.5
					φ	72.5	22.2	5.3
					γ_2	66.3	33.2	0.5
61	68.8	29.9	1.3	958	$Al_{11}Mn_4$	72.6	26.9	0.5
					φ	72.5	22.2	5.3
					γ_2	66.3	33.2	0.5
62	68.8	27.0	4.2	958	φ	71.5	21.8	6.7
					γ_2	65.4	33.6	1.0
63	71.5	22.3	6.2	90	φ	71.7	21.8	6.5
					γ_2	65.6	33.6	0.8
64	67.3	21.5	11.2	958	φ	69.3	21.1	9.6
					β	61.2	22.6	16.2
65	69.8	17.2	13.0	958	φ	70.6	18.5	10.9
					δ	60.9	2.2	36.9
66	68.6	11.2	20.2	958	φ	72.4	16.0	11.6
					δ	61.9	2.0	36.1
67	72.2	10.2	17.6	958	φ	73.6	14.2	12.2
					δ	63.2	1.8	35.0
					Al_3Ni	75.1	1.0	23.9
68	73.2	19.3	7.5	161	φ	73.2	19.3	7.5
69	75.9	21.7	2.4	161	$Al_{11}Mn_4$	72.7	26.8	0.5
					φ	76.3	21.2	2.5

Appendix (*Continued*)

No	Composition of alloy, at.%			Heat treatment, °C/h	Phase(s) in equilibrium	Phase composition, at.%		
	Al	Mn	Ni			Al	Mn	Ni
70	77.4	21.1	1.5	90	$Al_{11}Mn_4$	73.0	26.8	0.2
					φ	76.9	21.1	2.0
					μ	79.7	19.4	0.9
71	79.1	18.8	2.1	161	μ	79.7	19.2	1.1
					φ	77.1	21.1	2.8
					κ	79.4	18.1	2.5
72	76.5	18.3	5.2	161	φ	75.9	18.3	5.8
					κ	79.2	16.2	4.6
73	76.3	17.6	6.1	958	φ	75.8	18.0	6.2
					κ	79.1	15.9	5.0
74	78.4	15.5	6.1	161	φ	75.4	16.0	8.6
					κ	79.1	15.4	5.5
75	77.4	14.5	8.1	161	φ	75.4	14.8	9.8
					κ	79.0	15.1	5.9
					O	78.4	13.2	8.4
76	78.7	13.6	7.7	958	κ	79.4	14.8	5.8
					O	78.5	13.1	8.4
77	76.8	9.8	13.4	958	φ	75.1	13.9	11.0
					O	78.1	13.0	8.1
					Al_3Ni	75.3	1.1	23.6
78	80.1	7.0	12.9	90	O	78.2	12.8	9.0
					Al_3Ni	75.5	1.1	23.4
					L	~92.0	~4.0	~4.0
79	84.6	2.3	13.1	90	Al_3Ni	75.6	0.8	23.6
					L	~92.0	~3.5	~4.5
80	80.0	18.1	1.9	161	μ	80.1	18.8	1.1
					κ	79.9	18.2	1.9
81	83.1	15.8	1.1	958	μ	80.5	18.4	1.1
					L	~94.5	~4.0	~1.5
82	85.2	12.3	2.5	958	κ	80.4	17.2	2.4
					L	~94.0	~4.5	~1.5
83	84.6	12.5	2.9	161	κ	80.1	16.8	3.1
					L	~93.5	~4.0	~2.5
84	81.6	13.3	5.1	161	κ	79.8	14.8	5.4
					L	~93.0	~4.0	~3.0
85	81.2	11.6	7.2	161	κ	79.6	14.7	5.7
					O	78.6	13.0	8.4
					L	~93.0	~4.0	~3.0
700 °C								
86	76.6	23.4	–	372	$Al_{11}Mn_4$	73.1	26.9	–
					μ	79.1	20.9	–
87	80.5	19.5	–	372	μ	80.5	19.5	–
88	75.6	21.5	2.9	372	φ	75.6	21.5	2.9
89	77.5	20.7	1.8	372	$Al_{11}Mn_4$	73.0	26.8	0.2
					μ	79.5	19.8	0.7
					φ	76.7	22.1	1.2
90	78.9	19.5	1.6	372	μ	80.0	19.1	0.9
					κ	79.9	17.9	2.2
					φ	77.0	21.1	1.9
91	80.4	17.2	2.4	372	κ	80.4	17.2	2.4
92	78.1	17.3	4.6	372	κ	79.4	16.1	4.5
					φ	75.8	19.1	5.1
93	76.0	17.3	6.7	372	κ	79.3	15.7	5.0
					φ	75.5	17.4	7.1
94	77.1	15.2	7.7	372	κ	79.1	15.1	5.8
					φ	75.2	15.7	9.1
					O	78.3	13.2	8.5
95	78.4	14.0	7.6	372	κ	79.1	15.1	5.8
					φ	75.2	15.7	9.1
					O	78.3	13.2	8.5
96	78.9	13.0	8.1	372	O	78.9	13.0	8.1
97	72.6	10.8	16.6	372	φ	74.1	14.6	11.3
					δ	63.0	1.6	35.4
					Al_3Ni	75.2	0.9	23.9
98	76.2	12.0	11.8	372	O	78.0	12.9	9.1
					φ	74.9	14.1	11.0
					Al_3Ni	75.3	0.8	23.9
99	78.8	6.4	14.8	372	O	78.7	12.7	8.6
					Al_3Ni	75.5	0.6	23.9
					L	~95.5	~1.0	~3.5
100	81.6	10.9	7.5	372	O	79.1	12.7	8.2
					L	~95.5	~1.0	~3.5

Appendix (*Continued*)

No	Composition of alloy, at.%			Heat treatment, °C/h	Phase(s) in equilibrium	Phase composition, at.%		
	Al	Mn	Ni			Al	Mn	Ni
101	85.6	9.8	4.6	372	κ	80.3	15.1	4.3
					O	79.6	12.9	7.5
					L	~95.7	~1.3	~3.0
102	84.8	12.5	2.7	372	κ	80.9	16.2	2.9
					L	~96.0	~2.0	~2.0
103	86.5	11.5	2.0	372	κ	81.0	16.8	2.2
					L	~96.5	~2.0	~1.5
104	84.0	15.3	0.7	372	μ	80.9	18.2	0.9
					Al_6Mn	86.0	13.6	0.4
					L	~97.0	~2.5	~0.5
645 °C								
105	79.4	18.5	2.1	480	μ	80.0	18.6	1.4
					κ	80.0	17.4	2.6
					φ	76.8	21.4	1.8
106	79.7	18.5	1.8	336	μ	80.0	18.6	1.4
					κ	80.0	17.4	2.6
					φ	76.8	21.4	1.8
107	77.8	17.1	5.1	480	κ	78.9	16.1	5.0
					φ	75.8	19.0	5.2
108	78.2	14.2	7.6	480	O	78.0	13.8	8.2
					κ	79.1	15.4	5.5
109	79.6	15.1	5.3	480	O	79.4	13.6	7.0
					κ	79.8	15.3	4.9
110	80.8	14.4	4.8	480	O	81.0	13.4	5.6
					κ	80.5	15.1	4.4
					L	~96.0	~1.5	~2.5
111	76.1	11.2	12.7	480	O	77.4	13.2	9.4
					φ	74.9	15.6	9.5
					Al_3Ni	75.2	0.8	24.0
112	80.9	11.2	7.9	480	O	80.6	13.1	6.3
					Al_3Ni	75.5	0.6	23.9
					L	~96.0	~1.0	~3.0
113	79.1	6.7	14.2	480	O	80.6	13.1	6.3
					Al_3Ni	75.5	0.6	23.9
					L	~96.0	~1.0	~3.0
114	84.9	2.2	12.9	332	O	80.6	13.1	6.3
					Al_3Ni	75.5	0.6	23.9
					L	~96.0	~1.0	~3.0
115	95.8	0.6	3.6	332	Al_3Ni	75.4	0.4	24.2
					L	~96.5	~0.5	~3.0
116	95.1	1.9	3.0	332	O	80.9	13.1	6.0
					L	~96.0	~1.2	~2.8
117	95.1	2.9	2.0	332	κ	80.8	15.8	3.4
					(Al)	99.1	0.7	0.2
					L	~97.0	~1.0	~2.0
118	97.9	0.9	1.2	332	κ	80.8	15.8	3.4
					(Al)	99.1	0.7	0.2
					L	~97.0	~1.0	~2.0
119	95.4	3.7	0.9	332	κ	80.9	15.8	3.3
					(Al)	99.1	0.6	0.3
120	84.3	14.5	1.2	480	κ	81.0	16.2	2.8
					Al_6Mn	85.9	13.7	0.4
121	81.4	17.2	1.4	336	κ	81.0	16.6	2.4
					λ	81.2	17.9	0.9
					Al_6Mn	86.0	13.7	0.3
620 °C								
122	91.1	8.3	0.6	430	κ	80.9	15.8	3.3
					Al_6Mn	86.0	13.6	0.4
					(Al)	99.2	0.6	0.2
123	89.5	8.1	2.4	430	κ	80.6	15.5	3.9
					O	80.6	13.5	5.9
					(Al)	99.2	0.4	0.4
124	93.0	4.6	2.4	430	O	80.4	13.0	6.6
					(Al)	99.1	0.4	0.5
					Al_3Ni	75.5	23.9	0.6
125	92.9	4.3	2.8	430	O	80.4	13.0	6.6
					(Al)	99.1	0.4	0.5
					Al_3Ni	75.5	23.9	0.6
126	92.4	4.0	3.6	430	O	80.4	13.0	6.6
					(Al)	99.1	0.4	0.5
					Al_3Ni	75.5	23.9	0.6

Appendix (*Continued*)

No	Composition of alloy, at.%			Heat treatment, °C/h	Phase(s) in equilibrium	Phase composition, at.%		
	Al	Mn	Ni			Al	Mn	Ni
127	86.8	6.1	7.1	430	O	80.4	13.0	6.6
					(Al)	99.1	0.4	0.5
					Al_3Ni	75.5	23.9	0.6
128	81.8	6.8	11.4	430	O	80.4	13.0	6.6
					(Al)	99.1	0.4	0.5
					Al_3Ni	75.5	23.9	0.6
129	94.4	2.9	2.7	430	O	80.4	13.0	6.6
					(Al)	99.1	0.4	0.5
					Al_3Ni	75.5	23.9	0.6

L – solidified liquid.

References

[1] K. Urban, M. Feuerbacher, J. Non-Cryst. Sol. 334 (2003) 143.
[2] G.V.J. Raynor, Inst. Met. 70 (1944) 507.
[3] R. Kainuma, M. Ise, K. Ishikawa, I. Ohnuma, K. Ishida, J. Alloys Compd. 269 (1998) 173.
[4] C. Müller, H.H. Stadelmaier, B. Reinsch, G. Petzow, Z. Metallkd. 88 (1997) 620.
[5] D.J. Chakrabarti, Metall. Trans. B8 (1977) 121.
[6] S. Balanetskyy, G. Meisterernst, M. Feuerbacher, J Alloys Cmpd, (2010) in press.
[7] K. Robinson, Acta Cryst. 7 (1954) 494.
[8] T.B. Massalski (Ed.), Binary Alloy Phase Diagrams, vol. 2, ASM International, Materials-Park, OH, 1990, p. 970.
[9] G. Van Tendeloo, J. Van Landuyt, S. Amelinckx, S. Ranganathan, J. Microsc. 149 (1988) 1.
[10] A. Singh, S. Ranganathan, Mater. Sci. Eng. 754 (1994) A181–A182.
[11] H.X. Sui, K. Sun, K.H. Kuo, Phil. Mag. A75 (1997) 379.
[12] X.Z. Li, K.H. Kuo, Phill. Mag. Lett. 58 (1988) 167.
[13] M. Khaidar, C.H. Allibert, J. Driole, Z. Metallkd. 73 (1982) 433.
[14] S. Mi, B. Grushko, D. Dong, K. Urban, J. Alloys Compd. 351 (2003) L1.
[15] A.M.B. Douglas, Acta Cryst. 3 (1950) 19.
[16] V. Demange, J.S. Wu, V. Brien, F. Machizaud, J.M. Dubois, Mater. Sci. Eng. 294 (2000) 79.